Results in Physics 8 (2018) 365–371

Contents lists available at ScienceDirect

Results in Physics

journal homepage: www.journals.elsevier.com/results-in-physics

Viscous dissipation and Joule heating effects in MHD 3D flow with heat and mass fluxes

Taseer Muhammad [a,c,*], Tasawar Hayat [a,b], Sabir Ali Shehzad [d], Ahmed Alsaedi [b]

[a] Department of Mathematics, Quaid-I-Azam University, Islamabad 44000, Pakistan
[b] Nonlinear Analysis and Applied Mathematics (NAAM) Research Group, Department of Mathematics, Faculty of Science, King Abdulaziz University, Jeddah 21589, Saudi Arabia
[c] Department of Mathematics, Government College Women University, Sialkot 51310, Pakistan
[d] Department of Mathematics, COMSATS Institute of Information Technology, Sahiwal 57000, Pakistan

ARTICLE INFO

Article history:
Received 7 November 2017
Received in revised form 17 December 2017
Accepted 18 December 2017
Available online 20 December 2017

Keywords:
Three-dimensional flow
MHD
Flux conditions
Viscous dissipation
Joule heating
Exponentially stretching surface

ABSTRACT

The present research explores the three-dimensional stretched flow of viscous fluid in the presence of prescribed heat (PHF) and concentration (PCF) fluxes. Mathematical formulation is developed in the presence of chemical reaction, viscous dissipation and Joule heating effects. Fluid is electrically conducting in the presence of an applied magnetic field. Appropriate transformations yield the nonlinear ordinary differential systems. The resulting nonlinear system has been solved. Graphs are plotted to examine the impacts of physical parameters on the temperature and concentration distributions. Skin friction coefficients and local Nusselt and Sherwood numbers are computed and analyzed.

1. Introduction

The study of an electrically conducting fluid in view of its industrial and engineering applications is an important area of research for the investigators. It is well known fact that the final quality of product in manufacturing processes greatly depends on the cooling rate. A controlled cooling system is quite essential for such process. An electrically conducting fluid is the best candidate for applications in metallurgy, polymer technology and nuclear processes. In such processes the flow can be regulated by an applied magnetic field. Such applied magnetic field is quite useful to controlling momentum and heat transfer in boundary layer flows. Having such facts in mind, many authors have investigated the effect of applied magnetic field in flows through different flow configurations. Chen [1] investigated the effect of an applied magnetic field on the boundary layer flow of second grade and Walter's B liquids in the presence of thermal radiation. Analytical treatment of mixed convection flow of MHD viscoelastic fluid over a permeable stretching surface is made by Turkyilmazoglu [2]. Rashidi et al. [3] analyzed the entropy generation analysis in MHD slip flow of rotating viscous fluid with variable characteristics. An applied magnetic field effect on Falkner-Skan flow of Maxwell fluid via Chebyshev collocation method is examined by Abbasbandy et al. [4]. Seini and Makinde [5] discussed the magnetohydrodynamic boundary layer flow due to an exponentially stretching sheet. Hayat et al. [6] presented the series solutions of MHD three-dimensional flow of Maxwell fluid with variable thermal conductivity. Further recent investigations on MHD flows can be quoted through the studies [7–16].

The investigations through simultaneous effects of heat and mass transfer in the stretching flows are very popular subject amongst the recent researchers. Such analyses have potential role in the industrial and engineering processes like refrigeration and air conditioning, solar power collectors, damage of crops, desalination, human transpiration and many others [17–21]. Turkyilmazoglu [22] presented an analysis to study the combined effects of heat and mass transfer in the boundary layer flow of viscous nanofluid. Hayat et al. [23] developed the homotopic solutions for steady flow of Casson fluid with heat and mass transfer under thermal-diffusion and diffusion-thermo effects. Hayat and Alsaedi [24] studied the thermophoretic effects in boundary layer flow of an Oldroyd-B fluid with mixed convection. Shehzad et al. [25] extended the analysis of study [24] for a Jeffrey fluid model and provided the series solutions.

Joule heating is also known as ohmic heating. It is a mechanism by which the passage of an electric current through a conductor

* Corresponding author at: Department of Mathematics, Quaid-I-Azam University, Islamabad 44000, Pakistan.
E-mail address: taseer@math.qau.edu.pk (T. Muhammad).

https://doi.org/10.1016/j.rinp.2017.12.047
2211-3797/

produces heat. Joule heating has a variety of usage in industrial and technological processes such as electric stoves, electric heaters, incandescent light bulb, electric fuses, electronic cigarette, thermistor, food processing and several others. Thus Rahman [26] examined convective flow of micropolar fluid past a vertical radiate isothermal permeable surface with viscous dissipation and Joule heating. Hayat et al. [27] discussed non-uniform melting heat transfer effects in boundary-layer flow of nanofluid with viscous dissipation and Joule heating. Sheikholeslami and Ganji [28] studied magnetohydrodynamic flow of nanofluid between two parallel vertical permeable sheets with viscous dissipation and Joule heating. Mahanthesh et al. [29] addressed unsteady magnetohydrodynamic three-dimensional flow of Eyring-Powell nanofluid with viscous dissipation and Joule heating. Khan et al. [30] examined chemically reactive flow of micropolar fluid with viscous dissipation and Joule heating.

The cheaper raw materials are converted into higher standard products in chemically industrial processes. Such chemical reactions are made in a reactor. To provide a suitable environment to finishing products, a chemical reaction plays major role. Chemical reaction effects are quite prominent in petroleum reservoirs, chemical catalytic reactors, nuclear waste repositories, spreading of chemical pollutants, diffusion of medicine in blood veins etc. Hayat et al. [31] investigated the unsteady flow of third grade fluid over a stretching surface in the presence of chemical reaction. MHD mixed convection flow past a vertical porous plate embedded in a porous medium with thermal radiation and chemical reaction is examined by Makinde [32]. Rashidi et al. [33] discussed the group theoretic and differential transform analyses of mixed convective heat and mass transfer from a horizontal surface with chemical reaction. Effects of mass transfer on MHD flow of Casson fluid with chemical reaction and suction is examined by Shehzad et al. [34]. Mukhopadhyay and Vajravelu [35] studied the diffusion of chemically reactive species in Casson fluid flow by an unsteady permeable stretching surface.

The prime objective of present attempt is to explore the magnetohydrodynamic (MHD) three-dimensional flow of viscous fluid in the presence of chemical reaction, Joule heating and viscous dissipation. Flow is induced due to an exponentially stretching surface. Prescribed heat flux (PHF) and prescribed concentration flux (PCF) conditions are taken at the surface. To the best of our knowledge, no such consideration for three-dimensional flow of viscous fluid is given in the literature yet. Mathematical formulation is presented for both prescribed heat flux (PHF) and prescribed concentration flux (PCF) conditions (see [36–40]). Homotopy analysis method (HAM) [41–50] is applied for the solution development. Infact homotopy analysis method (HAM) has three advantages. Firstly it does not require small/large physical parameters in the problem. Secondly it provides a simple way to ensure the convergence of series solutions. Thirdly it provides a large freedom to choose the base functions and related auxiliary linear operators. Plots of physical quantities are presented and discussed. Further the skin-friction coefficients and local Nusselt and Sherwood numbers are computed and analyzed.

2. Mathematical modeling

We consider the steady three-dimensional flow of an incompressible viscous fluid. The fluid is caused by an exponentially stretching surface. Magnetic field of strength B_0 is applied in the z-direction. Induced magnetic field is not considered for small magnetic Reynolds number. A Cartesian coordinate system is chosen in such a manner that x- and y-axes are taken along the stretching surface and z-axis is normal to it. The sheet at $z=0$ is stretched in the x- and y-directions with velocities U_w and V_w respectively. Chemical reaction, viscous dissipation and Joule heating effects are taken into account. The thermophysical properties of fluid are taken constant. The governing boundary-layer expressions for three-dimensional flow of viscous fluid in the absence of thermal radiation are

$$\frac{\partial u}{\partial x}+\frac{\partial v}{\partial y}+\frac{\partial w}{\partial z}=0, \tag{1}$$

$$u\frac{\partial u}{\partial x}+v\frac{\partial u}{\partial y}+w\frac{\partial u}{\partial z}=\nu\frac{\partial^2 u}{\partial z^2}-\frac{\sigma B_0^2}{\rho}u, \tag{2}$$

$$u\frac{\partial v}{\partial x}+v\frac{\partial v}{\partial y}+w\frac{\partial v}{\partial z}=\nu\frac{\partial^2 v}{\partial z^2}-\frac{\sigma B_0^2}{\rho}v, \tag{3}$$

$$u\frac{\partial T}{\partial x}+v\frac{\partial T}{\partial y}+w\frac{\partial T}{\partial z}=\alpha\frac{\partial^2 T}{\partial z^2}+\frac{\sigma B_0^2}{\rho c_p}(u^2+v^2)+\frac{\mu}{\rho c_p}\left(\left(\frac{\partial u}{\partial z}\right)^2+\left(\frac{\partial v}{\partial z}\right)^2\right), \tag{4}$$

$$u\frac{\partial C}{\partial x}+v\frac{\partial C}{\partial y}+w\frac{\partial C}{\partial z}=D\frac{\partial^2 C}{\partial z^2}-K_1(C-C_\infty). \tag{5}$$

The boundary conditions for the present flow analysis are

$$\begin{aligned} &u=U_w=U_0e^{\frac{x+y}{L}},\ v=V_w=V_0e^{\frac{x+y}{L}},\ w=0, \quad \text{at } z=0;\\ &u\to 0,\ v\to 0 \quad \text{when } z\to\infty. \end{aligned} \tag{6}$$

The boundary conditions for the prescribed heat flux (PHF) and prescribed concentration flux (PCF) are imposed as follows:

$$\text{PHF}: -k\left(\frac{\partial T}{\partial z}\right)_w=T_0e^{\frac{(A+1)(x+y)}{2L}} \quad \text{at } z=0 \text{ and } T\to T_\infty \quad \text{when } z\to\infty, \tag{7}$$

$$\text{PCF}: -D\left(\frac{\partial C}{\partial z}\right)_w=C_0e^{\frac{(B+1)(x+y)}{2L}} \quad \text{at } z=0 \text{ and } C\to C_\infty \quad \text{when } z\to\infty, \tag{8}$$

where u, v and w are the velocity components in the x-, y- and z-directions respectively, $\nu=\mu/\rho$ the kinematic viscosity, μ the dynamic viscosity, ρ the density of fluid, σ the electrical conductivity, T the temperature, $\alpha=k/\rho c_p$ the thermal diffusivity of the fluid, k the thermal conductivity, c_p the specific heat at constant pressure, C the concentration, D the diffusion coefficient, K_1 the reaction rate, U_0, V_0, T_0 and C_0 the constants, L the reference length, A the temperature exponent, B the concentration exponent, T_w and T_∞ the temperatures of the surface and far away from the surface and C_w and C_∞ the concentrations at the surface and far away from the surface. The subscript w denotes the wall condition. The dimensionless variables can be defined as

$$\left.\begin{aligned} &u=U_0e^{\frac{x+y}{L}}f'(\eta),\ v=U_0e^{\frac{x+y}{L}}g'(\eta),\ w=-\left(\frac{\nu U_0}{2L}\right)^{1/2}e^{\frac{x+y}{2L}}(f+\eta f'+g+\eta g'),\\ &T=T_\infty+\frac{T_0}{k}\sqrt{\frac{2\nu L}{U_0}}e^{\frac{A(x+y)}{2L}}\theta(\eta),\ C=C_\infty+\frac{C_0}{D}\sqrt{\frac{2\nu L}{U_0}}e^{\frac{B(x+y)}{2L}}\phi(\eta),\ \eta=\left(\frac{U_0}{2\nu L}\right)^{1/2}e^{\frac{x+y}{2L}}z. \end{aligned}\right\} \tag{9}$$

Eq. (1) is automatically satisfied and Eqs. (2)–(8) have the following forms

$$f'''+(f+g)f''-2(f'+g')f'-M^2f'=0, \tag{10}$$

$$g'''+(f+g)g''-2(f'+g')g'-M^2g'=0, \tag{11}$$

$$\theta''+\Pr\left((f+g)\theta'-A(f'+g')\theta+M^2Ec\left(f'^2+g'^2\right)+Ec\left(f''^2+g''^2\right)\right)=0, \tag{12}$$

$$\phi'' + Sc((f+g)\phi' - B(f'+g')\phi - \gamma\phi) = 0, \tag{13}$$

$$f = 0, g = 0,\ f' = 1,\ g' = \beta,\ \theta' = -1,\ \phi' = -1 \quad \text{at } \eta = 0, \tag{14}$$

$$f' \to 0,\ g' \to 0,\ \theta \to 0,\ \phi \to 0 \quad \text{as } \eta \to \infty, \tag{15}$$

where M is the magnetic parameter, β the ratio parameter, Pr the Prandtl number, Ec the Eckert number, Sc the Schmidt number, γ the chemical reaction parameter and prime stands for differentiation with respect to η. These parameters can be defined as follows:

$$\left.\begin{aligned} &M^2 = \tfrac{2\sigma B_0^2 L}{\rho U_w},\ \beta = \tfrac{V_0}{U_0},\ \mathrm{Pr} = \tfrac{\nu}{\alpha},\\ &Ec = \tfrac{U_w^2}{c_p(T_w - T_\infty)},\ Sc = \tfrac{\nu}{D},\ \gamma = \tfrac{2K_1 L}{U_w}. \end{aligned}\right\} \tag{16}$$

The dimensionless skin friction coefficients along the x- and y-directions are given by

$$C_{fx} = \frac{\tau_{wx}|_{z=0}}{1/2\rho U_w^2} = \left(\frac{\mathrm{Re}}{2}\right)^{-1/2} f''(0), \tag{17}$$

$$C_{fy} = \frac{\tau_{wy}|_{z=0}}{1/2\rho U_w^2} = \left(\frac{\mathrm{Re}}{2}\right)^{-1/2} g''(0). \tag{18}$$

The local Nusselt number Nu_x and the local Sherwood number Sh_x are defined as

$$Nu_x = -\frac{x}{(T - T_\infty)}\frac{\partial T}{\partial z}\bigg|_{z=0} = \frac{x}{L}\left(\frac{\mathrm{Re}}{2}\right)^{1/2}\frac{1}{\theta(0)}, \tag{19}$$

$$Sh_x = -\frac{x}{(C - C_\infty)}\frac{\partial C}{\partial z}\bigg|_{z=0} = \frac{x}{L}\left(\frac{\mathrm{Re}}{2}\right)^{1/2}\frac{1}{\phi(0)}, \tag{20}$$

in which $\mathrm{Re} = U_w L/\nu$ is the local Reynolds number.

3. Series solutions

The initial guesses and the linear operators are

$$f_0(\eta) = 1 - e^{-\eta},\ g_0(\eta) = \beta(1 - e^{-\eta}),\ \theta_0(\eta) = e^{-\eta},\ \phi_0(\eta) = e^{-\eta}, \tag{21}$$

$$\mathcal{L}_f = f'''' - f',\ \mathcal{L}_g = g''' - g',\ \mathcal{L}_\theta = \theta'' - \theta,\ \mathcal{L}_\phi = \phi'' - \phi. \tag{22}$$

The above operators satisfy the properties given below:

$$\left.\begin{aligned} &\mathcal{L}_f[C_1 + C_2 e^{\eta} + C_3 e^{-\eta}] = 0,\ \mathcal{L}_g[C_4 + C_5 e^{\eta} + C_6 e^{-\eta}] = 0,\\ &\mathcal{L}_\theta[C_7 e^{\eta} + C_8 e^{-\eta}] = 0,\ \mathcal{L}_\phi[C_9 e^{\eta} + C_{10} e^{-\eta}] = 0, \end{aligned}\right\} \tag{23}$$

in which C_i $(i = 1 - 10)$ elucidate the arbitrary constants. We can define the following zeroth-order deformation problems

$$(1-p)\mathcal{L}_f\left[\hat{f}(\eta;p) - f_0(\eta)\right] = p\hbar_f \mathcal{N}_f[\hat{f}(\eta;p), \hat{g}(\eta;p)], \tag{24}$$

$$(1-p)\mathcal{L}_g[\hat{g}(\eta;p) - g_0(\eta)] = p\hbar_g \mathcal{N}_g[\hat{f}(\eta;p), \hat{g}(\eta;p)], \tag{25}$$

$$(1-p)\mathcal{L}_\theta\left[\hat{\theta}(\eta;p) - \theta_0(\eta)\right] = p\hbar_\theta \mathcal{N}_\theta[\hat{f}(\eta;p), \hat{g}(\eta;p), \hat{\theta}(\eta;p)], \tag{26}$$

$$(1-p)\mathcal{L}_\phi\left[\hat{\phi}(\eta;p) - \phi_0(\eta)\right] = p\hbar_\phi \mathcal{N}_\phi[\hat{f}(\eta;p), \hat{g}(\eta;p), \hat{\phi}(\eta;p)], \tag{27}$$

$$\left.\begin{aligned} &\hat{f}(0,p) = 0,\ \hat{f}'(0,p) = 1,\ \hat{f}'(\infty,p) = 0,\ \hat{g}(0,p) = 0,\ \hat{g}'(0,p) = \beta,\\ &\hat{g}'(\infty,p) = 0,\ \hat{\theta}'(0,p) = -1,\ \hat{\theta}(\infty,p) = 0,\ \hat{\phi}'(0,p) = -1,\ \hat{\phi}(\infty,p) = 0, \end{aligned}\right\} \tag{28}$$

$$\mathcal{N}_f\left[\hat{f}(\eta;p), \hat{g}(\eta;p)\right] = \frac{\partial^3 \hat{f}}{\partial \eta^3} + \left(\hat{f} + \hat{g}\right)\frac{\partial^2 \hat{f}}{\partial \eta^2} - 2\left(\frac{\partial \hat{f}}{\partial \eta} + \frac{\partial \hat{g}}{\partial \eta}\right)\frac{\partial \hat{f}}{\partial \eta} - M^2\frac{\partial \hat{f}}{\partial \eta}, \tag{29}$$

$$\mathcal{N}_g\left[\hat{g}(\eta;p), \hat{f}(\eta;p)\right] = \frac{\partial^3 \hat{g}}{\partial \eta^3} + \left(\hat{f} + \hat{g}\right)\frac{\partial^2 \hat{g}}{\partial \eta^2} - 2\left(\frac{\partial \hat{f}}{\partial \eta} + \frac{\partial \hat{g}}{\partial \eta}\right)\frac{\partial \hat{g}}{\partial \eta} - M^2\frac{\partial \hat{g}}{\partial \eta}, \tag{30}$$

$$\mathcal{N}_\theta\left[\hat{\theta}(\eta,p), \hat{f}(\eta;p), \hat{g}(\eta;p)\right] = \frac{\partial^2 \hat{\theta}}{\partial \eta^2} + \mathrm{Pr}\left(\begin{aligned} &\left(\hat{f} + \hat{g}\right)\tfrac{\partial \hat{\theta}}{\partial \eta} - A\left(\tfrac{\partial \hat{f}}{\partial \eta} + \tfrac{\partial \hat{g}}{\partial \eta}\right)\hat{\theta}\\ &+M^2 Ec\left(\left(\tfrac{\partial \hat{f}}{\partial \eta}\right)^2 + \left(\tfrac{\partial \hat{g}}{\partial \eta}\right)^2\right)\\ &+Ec\left(\left(\tfrac{\partial^2 \hat{f}}{\partial \eta^2}\right)^2 + \left(\tfrac{\partial^2 \hat{g}}{\partial \eta^2}\right)^2\right) \end{aligned}\right), \tag{31}$$

$$\mathcal{N}_\phi[\hat{\phi}(\eta,p), \hat{f}(\eta;p), \hat{g}(\eta;p)] = \frac{\partial^2 \hat{\phi}}{\partial \eta^2} + Sc\left(\left(\hat{f} + \hat{g}\right)\frac{\partial \hat{\phi}}{\partial \eta} - B\left(\frac{\partial \hat{f}}{\partial \eta} + \frac{\partial \hat{g}}{\partial \eta}\right)\hat{\phi} - \gamma\hat{\phi}\right). \tag{32}$$

In above expressions p denotes the embedding parameter, $\hbar_f, \hbar_g, \hbar_\theta$ and $\hbar_\phi$ the non-zero auxiliary parameters and $\mathcal{N}_f, \mathcal{N}_g, \mathcal{N}_\theta$ and $\mathcal{N}_\phi$ the nonlinear operators. Setting $p = 0$ and $p = 1$ we have

$$\hat{f}(\eta;0) = f_0(\eta),\ \hat{f}(\eta;1) = f(\eta), \tag{33}$$

$$\hat{g}(\eta;0) = g_0(\eta),\ \hat{g}(\eta;1) = g(\eta), \tag{34}$$

$$\hat{\theta}(\eta,0) = \theta_0(\eta),\ \hat{\theta}(\eta,1) = \theta(\eta), \tag{35}$$

$$\hat{\phi}(\eta,0) = \phi_0(\eta),\ \hat{\phi}(\eta,1) = \phi(\eta). \tag{36}$$

When p varies from 0 to 1 then $\hat{f}(\eta;p)$, $\hat{g}(\eta;p)$, $\hat{\theta}(\eta,p)$ and $\hat{\phi}(\eta,p)$ vary from the initial guesses $f_0(\eta), g_0(\eta)$, $\theta_0(\eta)$ and $\phi_0(\eta)$ to the final solutions $f(\eta)$, $g(\eta)$, $\theta(\eta)$ and $\phi(\eta)$, respectively. Taylor series expansion gives

$$\hat{f}(\eta;p) = f_0(\eta) + \sum_{m=1}^{\infty} f_m(\eta)p^m,\ f_m(\eta) = \frac{1}{m!}\frac{\partial^m \hat{f}(\eta,p)}{\partial p^m}\bigg|_{p=0}, \tag{37}$$

$$\hat{g}(\eta;p) = g_0(\eta) + \sum_{m=1}^{\infty} g_m(\eta)p^m,\ g_m(\eta) = \frac{1}{m!}\frac{\partial^m \hat{g}(\eta,p)}{\partial p^m}\bigg|_{p=0}, \tag{38}$$

$$\hat{\theta}(\eta,p) = \theta_0(\eta) + \sum_{m=1}^{\infty} \theta_m(\eta)p^m,\ \theta_m(\eta) = \frac{1}{m!}\frac{\partial^m \hat{\theta}(\eta,p)}{\partial p^m}\bigg|_{p=0}, \tag{39}$$

$$\hat{\phi}(\eta,p) = \phi_0(\eta) + \sum_{m=1}^{\infty} \phi_m(\eta)p^m,\ \phi_m(\eta) = \frac{1}{m!}\frac{\partial^m \hat{\phi}(\eta,p)}{\partial p^m}\bigg|_{p=0}. \tag{40}$$

The convergence of Eqs. (37)–(40) strongly depends upon the suitable choices of $\hbar_f, \hbar_g, \hbar_\theta$ and $\hbar_\phi$. Considering that $\hbar_f, \hbar_g, \hbar_\theta$ and $\hbar_\phi$ are chosen in such a manner that Eqs. (37)–(40) converge at $p = 1$ then

$$f(\eta) = f_0(\eta) + \sum_{m=1}^{\infty} f_m(\eta), \tag{41}$$

$$g(\eta) = g_0(\eta) + \sum_{m=1}^{\infty} g_m(\eta), \tag{42}$$

$$\theta(\eta) = \theta_0(\eta) + \sum_{m=1}^{\infty} \theta_m(\eta), \tag{43}$$

$$\phi(\eta) = \phi_0(\eta) + \sum_{m=1}^{\infty} \phi_m(\eta). \tag{44}$$

The general expressions of solutions can be expressed below which involve $f_m^*(\eta)$, $g_m^*(\eta)$, $\theta_m^*(\eta)$ and $\phi_m^*(\eta)$ as the special functions.

$$f_m(\eta) = f_m^*(\eta) + C_1 + C_2 e^{\eta} + C_3 e^{-\eta}, \tag{45}$$

$$g_m(\eta) = g_m^*(\eta) + C_4 + C_5 e^{\eta} + C_6 e^{-\eta}, \tag{46}$$

$$\theta_m(\eta) = \theta_m^*(\eta) + C_7 e^{\eta} + C_8 e^{-\eta}, \tag{47}$$

$$\phi_m(\eta) = \phi_m^*(\eta) + C_9 e^{\eta} + C_{10} e^{-\eta}. \tag{48}$$

4. Convergence analysis

Eqs. (41)–(44) involve the auxiliary parameters $\hbar_f$, $\hbar_g$, $\hbar_\theta$ and $\hbar_\phi$. The proper values of these parameters are quite essential to construct the convergent solutions via homotopy analysis method. To choose the suitable values of $\hbar_f$, $\hbar_g$, $\hbar_\theta$ and $\hbar_\phi$, the $\hbar$-curves are drawn at 20th order of approximations. Figs. 1 and 2 clearly show that the convergence region lies within the domain $-1.0 \leqslant \hbar_f \leqslant -0.15, -1.0 \leqslant \hbar_g \leqslant -0.10, -1.0 \leqslant \hbar_\theta \leqslant -0.35$ and $-1.0 \leqslant \hbar_\phi \leqslant -0.30$. Further the presented solutions are convergent in the whole domain when $\hbar_f = \hbar_g = -0.6 = \hbar_\theta = \hbar_\phi$. Numerical values of $f''(0), g''(0), \theta''(0)$ and $\phi''(0)$ at different order of HAM approximations are examined in Table 1 when $M = \gamma = Ec = 0.3$, $\beta = 0.1$, $Sc = 0.7$, $\Pr = 1.2$, $A = 0.4 = B$ and $\hbar_f = \hbar_g = -0.6 = \hbar_\theta = \hbar_\phi$. From this Table it is noted that the values of

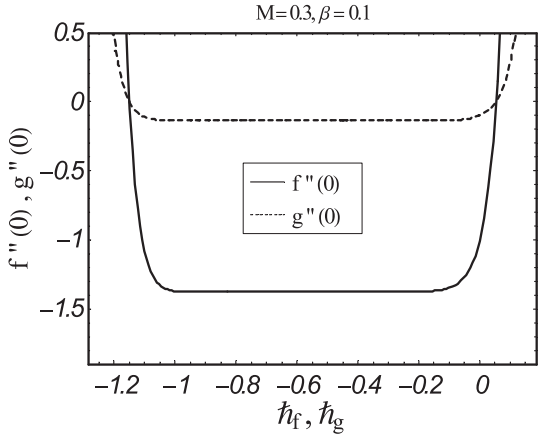

Fig. 1. $\hbar$-curves for $f(\eta)$ and $g(\eta)$.

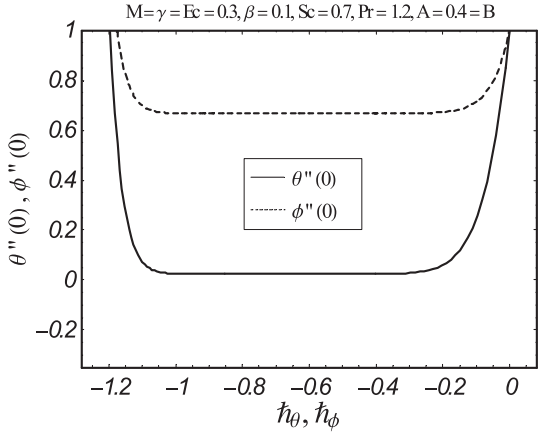

Fig. 2. $\hbar$-curves for $\theta(\eta)$ and $\phi(\eta)$.

Table 1
Numerical values of $-f''(0)$, $-g''(0)$, $\theta''(0)$ and $\phi''(0)$ for different order of approximations when $M = \gamma = Ec = 0.3$, $\beta = 0.1$, $Sc = 0.7$, $\Pr = 1.2$ and $A = 0.4 = B$.

Order of approximations	$-f''(0)$	$-g''(0)$	$\theta''(0)$	$\phi''(0)$
1	1.27700	0.12770	0.62067	0.80920
5	1.37665	0.13766	0.06888	0.67302
10	1.37812	0.13781	0.02458	0.66694
15	1.37812	0.13781	0.02318	0.66702
20	1.37812	0.13781	0.02310	0.66710
27	1.37812	0.13781	0.02309	0.66713
30	1.37812	0.13781	0.02309	0.66713
35	1.37812	0.13781	0.02309	0.66713
40	1.37812	0.13781	0.02309	0.66713

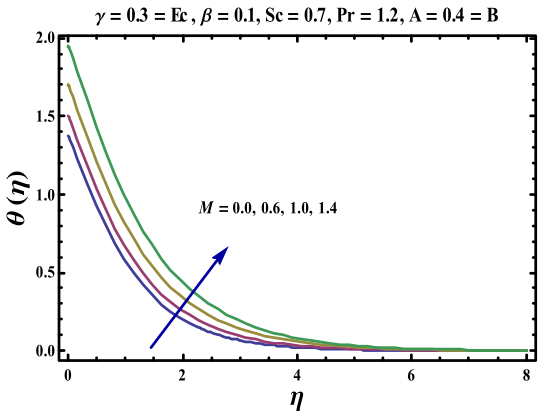

Fig. 3. Influence of M on $\theta(\eta)$.

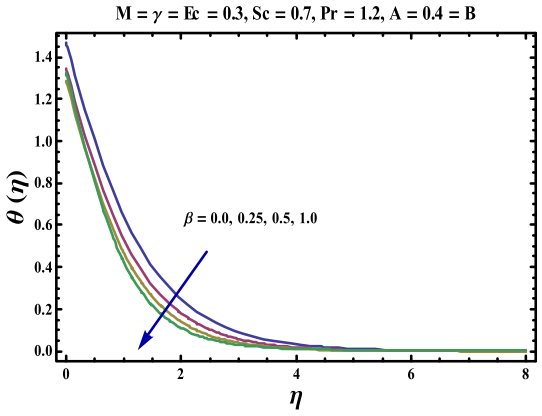

Fig. 4. Influence of β on $\theta(\eta)$.

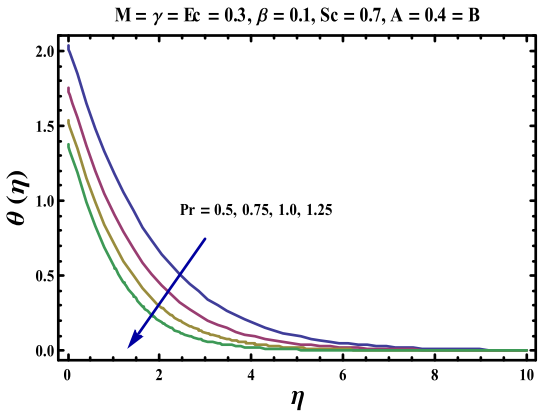

Fig. 5. Influence of Pr on $\theta(\eta)$.

$f''(0)$ and $g''(0)$ converge from 10th order of HAM deformations and the values of $\theta''(0)$ and $\phi''(0)$ converge from 27th order of HAM deformations. This Table concludes that 27th order of HAM iterations are essential for the convergent series solutions.

5. Results and discussion

Effects of magnetic parameter M, ratio parameter β, Prandtl number Pr, Eckert number Ec and temperature exponent A on the dimensionless temperature field $\theta(\eta)$ are examined in the Figs. 3–7. From Fig. 3 we have seen that the temperature profile is enhanced when we use the higher values of magnetic parameter. Lorentz force is involved in the magnetic parameter. Lorentz force is an agent which resists the fluid flow due to which more heat is produced and temperature is increased. Fig. 4 shows the impact of ratio parameter on the temperature field. Here we noticed that temperature and thermal boundary layer thickness are decreasing functions of ratio parameter. Fig. 5 elucidates that the temperature and thermal boundary layer thickness are reduced when we increase the values of Prandtl number. Prandtl number is inversely proportional to thermal diffusivity. Larger Prandtl number has weaker thermal diffusivity. Such weaker thermal diffusivity corresponds to a

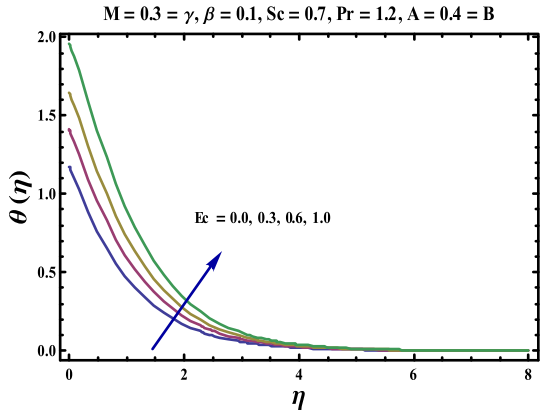

Fig. 6. Influence of Ec on $\theta(\eta)$.

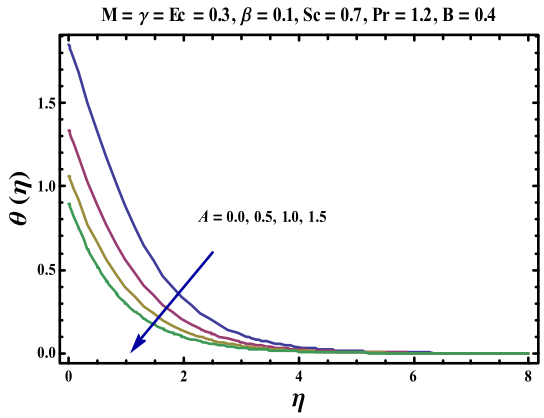

Fig. 7. Influence of A on $\theta(\eta)$.

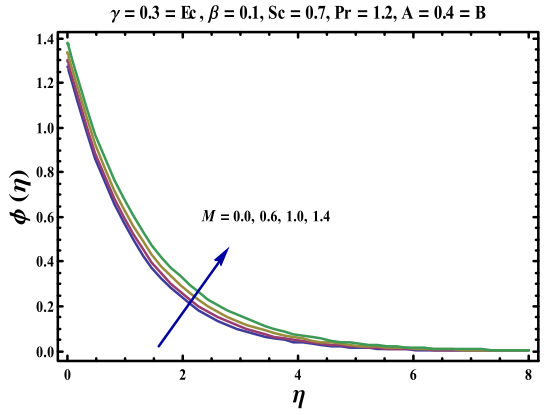

Fig. 8. Influence of M on $\phi(\eta)$.

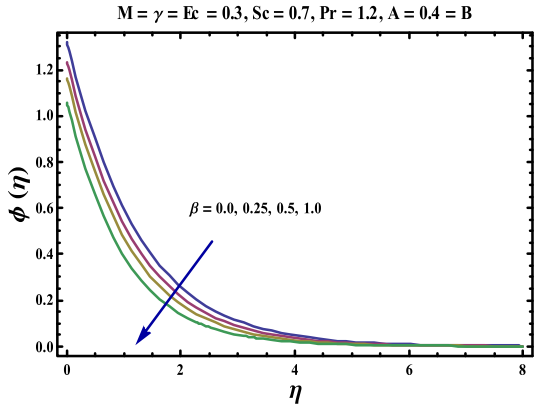

Fig. 9. Influence of β on $\phi(\eta)$.

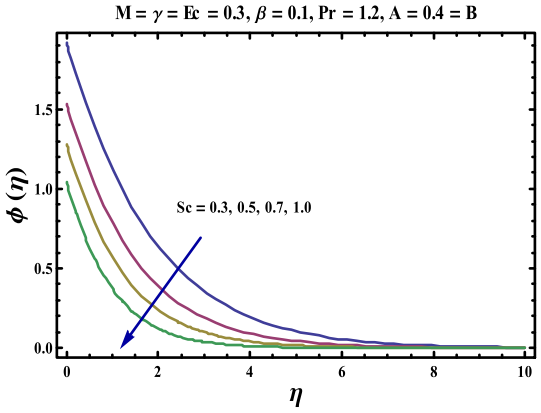

Fig. 10. Influence of Sc on $\phi(\eta)$.

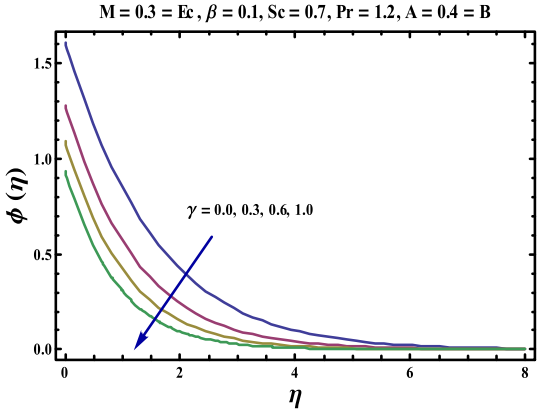

Fig. 11. Influence of γ on $\phi(\eta)$.

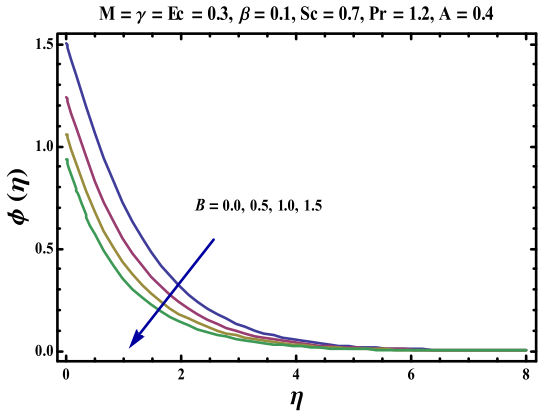

Fig. 12. Influence of B on $\phi(\eta)$.

Table 2
Numerical values of skin friction coefficients $-f''(0)$ and $-g''(0)$ for different values of M and β.

M	β	$-f''(0)$	$-g''(0)$
0.0	0.1	1.34439	0.13444
0.5		1.43592	0.14359
1.0		1.67900	0.16790
0.3	0.0	1.31716	0.00000
	0.3	1.49259	0.44778
	0.5	1.59890	0.79945

reduction in the temperature and thermal boundary layer thickness. An increase in temperature and thermal boundary layer thickness is observed for the larger values of Eckert number. Here the increasing values of Eckert number give rise to the temperature difference that leads to higher temperature and thermal boundary layer thickness (see Fig. 6). Fig. 7 illustrates the variation in temperature for various values of temperature exponential parameter. Smaller temperature exponent parameter corresponds to the higher temperature and thermal boundary layer thickness.

Figs. 8–12 are sketched to examine the behaviors of magnetic parameter M, ratio parameter β, Schmidt number Sc, chemical reaction parameter γ and concentration exponent B on the dimensionless concentration profile $\phi(\eta)$. Concentration and its related boundary layer thickness are increased for the larger magnetic parameter (see Fig. 8). Further $M = 0$ corresponds to hydrodynamic flow. Fig. 9 depicts that concentration is weak for larger ratio parameter. It is also noticed that when $\beta = 0$, the two-dimensional flow situation is achieved. Effects of Schmidt number on concentration profile are seen in Fig. 10. It is clearly indicates that concentration is decreased with an increase in the values of Schmidt number. Schmidt number depends on the diffusion coefficient. An increase in Schmidt number corresponds to weaker diffusion coefficient. This weaker diffusion coefficient shows a reduction in the concentration and its related boundary layer thickness. From Fig. 11 we observed that concentration profile is enhanced when we use larger values of chemical reaction parameter. Fig. 12 elucidates that concentration and its related boundary layer thickness are decreasing functions of concentration exponent.

Table 2 shows the numerical values of skin friction coefficients $f''(0)$ and $g''(0)$ for different values of $M$and β. Here we noticed that the skin friction coefficients are increased with the increase in M and β. It is also noticed that $\beta = 0$ corresponds to $g''(0) = 0$ which recovered the two-dimensional flow analysis. Table 3 presents the values of the local Nusselt number $\frac{1}{\theta(0)}$ and local Sherwood number $\frac{1}{\phi(0)}$ for various values of $M, \beta, \mathrm{Pr}, Ec, Sc$ and γ when $A = 0.4 = B$. From this Table we observed that the values of $\frac{1}{\theta(0)}$ and $\frac{1}{\phi(0)}$ are decreased with an increase in M. However these values are larger for higher β and Pr.

6. Conclusions

Effects of chemical reaction, viscous dissipation and Joule heating in magnetohydrodynamic (MHD) three-dimensional flow with prescribed heat flux (PHF) and prescribed concentration flux (PCF) are examined in this article. Important observations of present analysis are given below:

- An increase in magnetic parameter M gives rise to the temperature and concentration fields.
- Larger values of ratio parameter β decrease the temperature and concentration boundary layer thicknesses.
- An increase in the Prandtl number Pr decreases the temperature field.
- Concentration is a decreasing function of Schmidt number Sc.
- An increase in Eckert number Ec gives rise to the temperature field.
- Concentration is a decreasing function of chemical reaction parameter γ.

Table 3
Numerical values of local Nusselt number $\frac{1}{\theta(0)}$ and local Sherwood number $\frac{1}{\phi(0)}$ for different values of $M, \beta, \mathrm{Pr}, Ec, Sc$ and γ when $A = 0.4 = B$.

M	β	Pr	Ec	Sc	γ	$\frac{1}{\theta(0)}$	$\frac{1}{\phi(0)}$
0.0	0.1	1.2	0.3	0.7	0.3	0.72496	0.78110
0.5						0.67894	0.76885
1.0						0.57660	0.74020
0.3	0.0	1.2	0.3	0.7	0.3	0.67928	0.75472
	0.3					0.75046	0.81801
	0.5					0.77497	0.85728
0.3	0.1	1.0	0.3	0.7	0.3	0.64167	0.77648
		1.5				0.79033	0.77648
		2.0				0.89889	0.77648
0.3	0.1	1.2	0.0	0.7	0.3	0.84899	0.77648
			0.3			0.70742	0.77648
			0.5			0.63665	0.77648
0.3	0.1	1.2	0.3	0.5	0.3	0.70742	0.63472
				0.7		0.70742	0.77648
				1.0		0.70742	0.95929
0.3	0.1	1.2	0.3	0.7	0.0	0.70742	0.58550
					0.3	0.70742	0.77648
					0.5	0.70742	0.87317

- Temperature exponent A and concentration exponent B show similar behaviors on the temperature and concentration fields.

References

[1] Chen CH. On the analytic solution of MHD flow and heat transfer for two types of viscoelastic fluid over a stretching sheet with energy dissipation, internal heat source and thermal radiation. Int. J. Heat Mass Transfer 2010;53:4264–73.
[2] Turkyilmazoglu M. The analytical solution of mixed convection heat transfer and fluid flow of a MHD viscoelastic fluid over a permeable stretching surface. Int. J. Mech. Sci. 2013;77:263–8.
[3] Rashidi MM, Kavyani N, Abelman S. Investigation of entropy generation in MHD and slip flow over a rotating porous disk with variable properties. Int. J. Heat Mass Transfer 2014;70:892–917.
[4] Abbasbandy S, Hayat T, Ghehsareh HR, Alsaedi A. MHD Falkner-Skan flow of Maxwell fluid by rational Chebyshev collocation method. Appl. Math. Mech. Engl. Ed. 2013;34:921–30.
[5] Seini YI, Makinde OD. MHD boundary layer flow due to exponential stretching surface with radiation and chemical reaction. Math. Prob. Eng. 2013;2013:163614.
[6] Hayat T, Shehzad SA, Qasim M, Asghar S. Three-dimensional stretched flow via convective boundary condition and heat generation/absorption. Int. J. Numer. Methods Heat Fluid Flow 2014;24:342–58.
[7] Hayat T, Muhammad T, Shehzad SA, Chen GQ, Abbas IA. Interaction of magnetic field in flow of Maxwell nanofluid with convective effect. J. Magn. Magn. Mater. 2015;389:48–55.
[8] Hayat T, Aziz A, Muhammad T, Ahmad B. Influence of magnetic field in three-dimensional flow of couple stress nanofluid over a nonlinearly stretching surface with convective condition. PLoS One 2015;10:e0145332.
[9] Hayat T, Muhammad T, Qayyum A, Alsaedi A, Mustafa M. On squeezing flow of nanofluid in the presence of magnetic field effects. J. Mol. Liq. 2016;213:179–85.
[10] Alsaedi A, Hayat T, Muhammad T, Shehzad SA. MHD three-dimensional flow of viscoelastic fluid over an exponentially stretching surface with variable thermal conductivity. Comput. Math. Math. Phys. 2016;56:1665–78.
[11] Hayat T, Aziz A, Muhammad T, Ahmad B. On magnetohydrodynamic flow of second grade nanofluid over a nonlinear stretching sheet. J. Magn. Magn. Mater. 2016;408:99–106.
[12] Hayat T, Abbas T, Ayub M, Muhammad T, Alsaedi A. On squeezed flow of Jeffrey nanofluid between two parallel disks. Appl. Sci. 2016;6:346.
[13] Hayat T, Ullah I, Muhammad T, Alsaedi A. A revised model for stretched flow of third grade fluid subject to magneto nanoparticles and convective condition. J. Mol. Liq. 2017;230:608–15.
[14] Muhammad T, Hayat T, Alsaedi A, Qayyum A. Hydromagnetic unsteady squeezing flow of Jeffrey fluid between two parallel plates. Chin. J. Phys. 2017;55:1511–22.
[15] Hayat T, Haider F, Muhammad T, Alsaedi A. On Darcy-Forchheimer flow of viscoelastic nanofluids: a comparative study. J. Mol. Liq. 2017;233:278–87.
[16] Hayat T, Sajjad R, Ellahi R, Alsaedi A, Muhammad T. Homogeneous-heterogeneous reactions in MHD flow of micropolar fluid by a curved stretching surface. J. Mol. Liq. 2017;240:209–20.
[17] Hu Z, Lu W, Thouless MD. Slip and wear at a corner with Coulomb friction and an interfacial strength. Wear 2015;338:242–51.
[18] Hu Z, Lu W, Thouless MD, Barber JR. Simulation of wear evolution using fictitious eigenstrains. Tribol. Int. 2015;82:191–4.
[19] Hu Z, Thouless MD, Lu W. Effects of gap size and excitation frequency on the vibrational behavior and wear rate of fuel rods. Nucl. Eng. Des. 2016;308:261–8.
[20] Hu Z, Lu W, Thouless MD, Barber JR. Effect of plastic deformation on the evolution of wear and local stress fields in fretting. Int. J. Solids Struct. 2016;82:1–8.
[21] Wang H, Hu Z, Lu W, Thouless MD. The effect of coupled wear and creep during grid-to-rod fretting. Nucl. Eng. Des. 2017;318:163–73.
[22] Turkyilmazoglu M. Exact analytical solutions for heat and mass transfer of MHD slip flow in nanofluids. Chem. Eng. Sci. 2012;84:182–7.
[23] Hayat T, Shehzad SA, Alsaedi A. Soret and Dufour effects on magnetohydrodynamic (MHD) flow of Casson fluid. Appl. Math. Mech. Engl. Ed. 2012;33:1301–12.
[24] Hayat T, Alsaedi A. On thermal radiation and Joule heating effects in MHD flow of an Oldroyd-B fluid with thermophoresis. Arab. J. Sci. Eng. 2011;36:1113–24.
[25] Shehzad SA, Alsaedi A, Hayat T. Influence of thermophoresis and joule heating on the radiative flow of jeffrey fluid with mixed convection. Braz. J. Chem. Eng. 2013;30:897–908.
[26] Rahman MM. Convective flows of micropolar fluids from radiate isothermal porous surfaces with viscous dissipation and Joule heating. Commun. Nonlinear Sci. Numer. Simul. 2009;14:3018–30.
[27] Hayat T, Imtiaz M, Alsaedi A. Melting heat transfer in the MHD flow of Cu-water nanofluid with viscous dissipation and Joule heating. Adv. Powder Technol. 2016;27:1301–8.
[28] Sheikholeslami M, Ganji DD. Nanofluid hydrothermal behavior in existence of Lorentz forces considering Joule heating effect. J. Mol. Liq. 2016;224:526–37.
[29] Mahanthesh B, Gireesha BJ, Gorla RSR. Unsteady three-dimensional MHD flow of a nano Eyring-Powell fluid past a convectively heated stretching sheet in the presence of thermal radiation, viscous dissipation and Joule heating. J. Assoc. Arab Uni. Basic Appl. Sci. 2017;23:75–84.
[30] Khan MI, Waqas M, Hayat T, Alsaedi A. Chemically reactive flow of micropolar fluid accounting viscous dissipation and Joule heating. Results Phys. 2017;7:3706–15.
[31] Hayat T, Mustafa M, Asghar S. Unsteady flow with heat and mass transfer of a third grade fluid over a stretching surface in the presence of chemical reaction. Nonlinear Anals. Real World Appl. 2010;11:3186–97.
[32] Makinde OD. MHD mixed-convection interaction with thermal radiation and nth order chemical reaction past a vertical porous plate embedded in a porous medium. Chem. Eng. Commun. 2011;198:590–608.
[33] Rashidi MM, Rahimzadeh N, Ferdows M, Uddin MJ, B ég OA. Group theory and differential transform analysis of mixed convective heat and mass transfer from a horizontal surface with chemical reaction effects. Chem. Eng. Comm. 2012;199:1012–43.
[34] Shehzad SA, Hayat T, Qasim M, Asghar S. Effects of mass transfer on MHD flow of Casson Fluid with chemical reaction and suction. Braz. J. Chem. Eng. 2013;30:187–95.
[35] Mukhopadhyay S, Vajravelu K. Diffusion of chemically reactive species in Casson fluid flow over an unsteady permeable stretching surface. J. Hydrodynamics 2013;25:591–8.
[36] Abbasi FM, Shehzad SA, Hayat T, Alsaedi A, Obid MA. Influence of heat and mass flux conditions in hydromagnetic flow of Jeffrey nanofluid. AIP Adv. 2015;5:037111.
[37] Hayat T, Ullah I, Muhammad T, Alsaedi A, Shehzad SA. Three-dimensional flow of Powell-Eyring nanofluid with heat and mass flux boundary conditions. Chin. Phys. B 2016;25:074701.
[38] Hayat T, Ullah I, Alsaedi A, Ahmad B. Modeling tangent hyperbolic nanoliquid flow with heat and mass flux conditions. Eur. Phys. J. Plus 2017;132:112.
[39] Upadhay MS, Mahesha, Raju CSK. Cattaneo-Christov on heat and mass transfer of unsteady Eyring Powell dusty nanofluid over sheet with heat and mass flux conditions. Inf. Med. Unlocked 2017;9:76–85.
[40] Hayat T, Aziz A, Muhammad T, Alsaedi A. Three-dimensional flow of nanofluid with heat and mass flux boundary conditions. Chin. J. Phys. 2017;55:1495–510.
[41] Liao SJ. On the homotopy analysis method for nonlinear problems. Appl. Math. Comput. 2004;147:499–513.
[42] Dehghan M, Manafian J, Saadatmandi A. Solving nonlinear fractional partial differential equations using the homotopy analysis method. Numer. Meth. Partial Diff. Eq. 2010;26:448–79.
[43] Abbasbandy S, Hashemi MS, Hashim I. On convergence of homotopy analysis method and its application to fractional integro-differential equations. Quaestiones Mathematicae 2013;36:93–105.
[44] Hayat T, Muhammad T, Alsaedi A, Alhuthali MS. Magnetohydrodynamic three-dimensional flow of viscoelastic nanofluid in the presence of nonlinear thermal radiation. J. Magn. Magn. Mater. 2015;385:222–9.
[45] Abd Elmaboud Y, Mekheimer KhS, Mohamed MS. Series solution of a natural convection flow for a Carreau fluid in a vertical channel with peristalsis. J. Hydrodynamics Ser. B 2015;27:969–79.
[46] Turkyilmazoglu M. An effective approach for evaluation of the optimal convergence control parameter in the homotopy analysis method. Filomat 2016;30:1633–50.
[47] Awais M, Saleem S, Hayat T, Irum S. Hydromagnetic couple-stress nanofluid flow over a moving convective wall: OHAM analysis. Acta Astronaut. 2016;129:271–6.
[48] Hayat T, Aziz A, Muhammad T, Alsaedi A. On magnetohydrodynamic three-dimensional flow of nanofluid over a convectively heated nonlinear stretching surface. Int. J. Heat Mass Transfer 2016;100:566–72.
[49] Hayat T, Aziz A, Muhammad T, Alsaedi A. Active and passive controls of Jeffrey nanofluid flow over a nonlinear stretching surface. Results Phys. 2017;7:4071–8.
[50] Muhammad T, Alsaedi A, Shehzad SA, Hayat T. A revised model for Darcy-Forchheimer flow of Maxwell nanofluid subject to convective boundary condition. Chin. J. Phys. 2017;55:963–76.